Theoretical Study of Surface Plasmon Resonances in Hollow Gold−Silver Double-Shell Nanostructures†

Carlos E. Román-Velázquez,‡ Cecilia Noguez,*,‡ and Jin Z. Zhang§

Instituto de Física, Universidad Nacional Autónoma de México, Apartado Postal 20-364, México D.F. 01000, México, and Department of Chemistry and Biochemistry, University of California, Santa Cruz, California 95064

Received: November 27, 2009; Revised Manuscript Received: January 9, 2009

A theoretical model has been developed to study the optical properties of metallic multishell structures on the nanometer scale. The Mie theory was generalized for multiconcentric spherical shell nanostructures and employed to determine the effects and importance of the different parameters of the system such as thickness, size, and other material properties, for instance, the medium index of refraction. A unique hollow gold−silver double-shell structure is used as an example to test the model developed with recent experiments. The surface plasmon resonance (SPR) absorption spectrum of this structure has been calculated as a function of various parameters, including shell thickness and diameter. Using parameters similar to those previously reported experimentally, very good agreement has been found between calculated and experimentally measured SPR spectra, which validates the model. The results provide new insights into the fundamental properties of complex metal nanostructures that give us the ability to control the optical response, which has important implications in the synthesis of new metal nanostructures as well as their application in emerging technologies.

Introduction

Metal nanostructures exhibit a wide variety of interesting physical and chemical properties, which can be tailored by altering their size, morphology, composition, and environment.[1] The knowledge of and relationship among these parameters are relevant to the systematic synthesis of metal nanostructures with uniform and reliable properties and functionalities.[2] Theoretical and simulational studies play a major role in the explanation and prediction of novel nanostructures and are complementary to experimental studies.[3,4] One of the most fascinating aspects of nanosized metal structures is their optical property that finds various technological applications such as surface plasmon resonance detection and imaging,[5−9] surface-enhanced Raman scattering (SERS),[10−14] and biomedical imaging and therapy.[15,16]

The optical response of nanoparticles such as gold and silver exhibits strong absorption in the visible region of the spectrum and is mainly determined by their surface plasmon resonances (SPRs). The SPR absorption spectra are strongly dependent on the nanoparticle's geometry, composition, and surroundings. The origin of this absorption is attributed to collective conduction band electron oscillations in response to the electrical field of the incident electromagnetic radiation of light, displacing the electron cloud from the nuclei. The long-range correlation of electrons caused by Coulomb forces and the attraction between positive and negative charges result in a restoring force that changes the oscillation frequency of the electron cloud with respect to the positive nuclear background. In metallic particles, the collective motion of electrons produces surface modes, whose number, position, and width are determined by the particle's shape and variations of its dielectric function.[1] This optical absorption is termed surface plasmon resonance, partly because net charges are displaced transiently on the particle surface during electron oscillation.

Different shaped nanostructures possess vastly different absorption spectra or colors,[17−22] which are the result of multiple SPRs in complex structures, such as nanocages, aggregates, and nanoprisms that usually have more nondegenerate resonances than highly symmetric particles and thereby broad overall absorption spectrum.[23] The lower the symmetry the structure has, the more nondegenerate modes there are. In principle, almost any shape can be produced, including aggregates, nanorods, nanowires, nanocages, nanospheres, nanoprisms, and nanoplates or sheets, as reported in the literature.[24−32]

In addition to producing particles with nonspherical shapes, it is also possible to alter the internal structure of a particle to manipulate their optical properties. Dielectric/metal core/shell and hollow metal structures are good examples. For instance, the optical absorption can be managed in hollow nanoparticles by using different combinations of shell thickness and size diameter.[31] Furthermore, by using the hollow gold nanoparticles as seeds, it has been demonstrated to be possible to controllably grow a layer of silver with tunable thickness, resulting in the generation of unique hollow gold−silver double nanoshells.[33] The first thing to note of these double nanoshells is the significantly shifted and broadened plasmon band that can be tuned to some extent by controlling silver thickness. The plasmon absorption changes from predominantly that of gold to that of silver with increasing the silver coating as the outer shell. The double nanoshells have shown greatly increased Raman enhancement over hollow gold nanoparticles due likely to a combination of the increased overall volume of metal and the improved enhancement factor of silver over gold as the outer shell.[33] In addition, the unique combination of small size, spherical shape, as well as strong, tunable, and narrow SPR of hollow gold nanospheres (HGN or HAuNS) is ideal for

† Part of the "George C. Schatz Festschrift".
* Corresponding author, cecilia@fisica.unam.mx.
‡ Universidad Nacional Autónoma de México.
§ University of California, Santa Cruz.

10.1021/jp810422r CCC: $40.75
Published on Web 02/18/2009

SCHEME 1: Schematic Model of the Concentric Multishell Spherical Particle

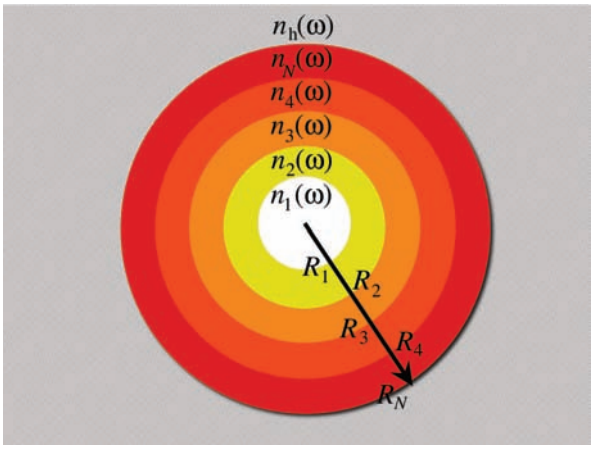

biomedical applications, as demonstrated successfully recently in both in vitro and in vivo photothermal ablation (PTA) therapy of cancer cells.[15,16]

In this work, an extended Mie theory is developed and implemented numerically to study metal double nanoshells in order to gain a better fundamental understanding of the optical properties of such complex nanostructures. The developed formalism is used to understand recent experimental data on the optical absorbance of hollow gold−silver double-shell nanoparticles. The importance of thickness of both shells and their diameters in the manipulation of the SPRs is discussed. The calculated data show excellent agreement with the experimental results. The model developed is expected to be useful in guiding the development of other complex metal nanostructures for different applications.

Theory

When a metal particle is subject to the action of an electromagnetic (EM) field, its electrons start to oscillate, transforming energy from the incident EM wave into, for example, thermal energy in a so-called absorption process. The electrons can also be accelerated, and then they can radiate energy in a so-called scattering process. In a typical experimental setup the attenuation by the sum of scattering and absorption of an electromagnetic wave going through a material is called the EM extinction. In this work, we consider a system composed of nanoparticles (NPs) dispersed in a homogeneous medium as a very dilute system. In the dilute limit, the interactions between particles are negligible, such that, the extinction of the whole sample, σ_{ext}, can be modeled as the optical response of one immersed NP times the concentration of particles[34]

$$\sigma_{ext} = nC_{ext} = n(C_{abs} + C_{sca}) \quad (1)$$

where n is the number of particles per unit volume, C_{ext} is the extinction cross section given by the sum of C_{abs} and C_{sca}, which are the absorption and scattering cross sections of a single particle. In 1908, Gustav Mie found the exact solution to the Maxwell equations for the optical response of a sphere of arbitrary size immersed in a homogeneous medium, subject to a plane monochromatic wave.[35] In this case, the optical cross sections were developed in terms of the electric field and magnetic vector, which are given in series of the Legendre polynomials and Bessel spherical functions.[34] Here, we extend the Mie theory to consider a spherical NP composed by an arbitrary number of shells of different refraction indexes, which is immersed in a host medium with arbitrary dielectric properties.

Consider a multishell spherical nanoparticle that consists of N concentric spherical surfaces of external radius R_i. The NP is immersed in a host medium (for $r > R_N$) with a refraction index n_h. The first shell finishes at $r = R_1$ and is named the core or hollow, depending of the kind of NP. The core and the other $N - 1$ shells can be made of different materials characterized by frequency depending refraction indexes $n_i(\omega)$. A schematic model of a NP composed by a core and four shells immersed in a host medium is shown in Scheme 1.

Now, let us consider that the multishell nanoparticle is excited by a plane electromagnetic wave that is polarized along the $\hat{x}$ axis and propagates in the direction with $\theta = 0$. Each region of the system is described by a radial coordinate variable such that $R_i < r \leq R_{i+1}$, where r takes values from 0 to ∞, and $i = 0,..., N + 1$, where $R_0 = 0$, and R_{N+1} corresponds to a point in the host medium. Then, the scattered electromagnetic field is given by

$$\mathbf{E} = \nabla \times \mathbf{r}\Psi^{(m)} - \frac{i}{k}\nabla \times (\nabla \times \mathbf{r}\Psi^{(e)}) \quad (2)$$

$$\mathbf{H} = -n_i \nabla \times \mathbf{r}\Psi^{(e)} - n_i \frac{i}{k}\nabla \times (\nabla \times \mathbf{r}\Psi^{(m)}) \quad (3)$$

where n_i is the refraction index of the propagating medium, $k = n\omega/c$ is the amplitude of the wave vector, and c is the speed of light. Here, $\Psi_i^{(e)}$ is the Debye potential corresponding to the transverse magnetic field and $\Psi_i^{(m)}$ corresponds to the transverse electric field. Both potentials satisfy the scalar Hemholtz equation (7) that have solutions, as shown in the Appendix, of the following form

$$\Psi_i^{(e)}(r, \theta, \varphi) = \sum_{l=1}^{\infty} \{a_l^i h_l(kr) + b_l^i j_l(kr)\} P_l^1(\cos\theta) \cos\varphi \quad (4)$$

$$\Psi_i^{(m)}(r, \theta, \varphi) = \sum_{l=1}^{\infty} \{c_l^i h_l(kr) + d_l^i j_l kr\} P_l^1(\cos\theta) \sin\varphi \quad (5)$$

where $h_l = j_l + iy_l$ are the spherical Hankel functions, j_l and y_l are the spherical Bessel functions of first and second kind, respectively, P_l^1 are the associated Legendre Polynomials with $m = 1$, and a_l^i, b_l^i, c_l^i, and d_l^i, are the coefficients of the expansions in eqs 4 and 5, which are found by solving the linear system of equations given by the boundary conditions of the EM field, as shown in the Appendix.

Then the scattering field characterized by the extinction cross section C_{ext} is found to be[36]

$$C_{ext} = \frac{\lambda^2}{2\pi}\sum_{l=1}^{\infty}(2l+1)\mathrm{Re}[\alpha_l + \beta_l] \quad (6)$$

where the coefficients $\alpha_l = a_l^{N+1}/b_l^{N+1}$, and $\beta_l = c_l^{N+1}/d_l^{N+1}$ correspond to the ratio between the scattered EM field from the particle in the host medium and the incident EM field.

Thus, we have developed a theoretical model to study the optical response of a multishell spherical particle of arbitrary size. Previous work has been developed in this direction to study this system, like the plasmon hybridization model where the interaction between surface plasmons can be seen as the hybridization of the free excitations of the cavity and the sphere.[37] The plasmon hybridization model was developed in

SCHEME 2: Schematic Model of the Hollow Gold−Silver Double-Shell Nanoparticle Studied Here

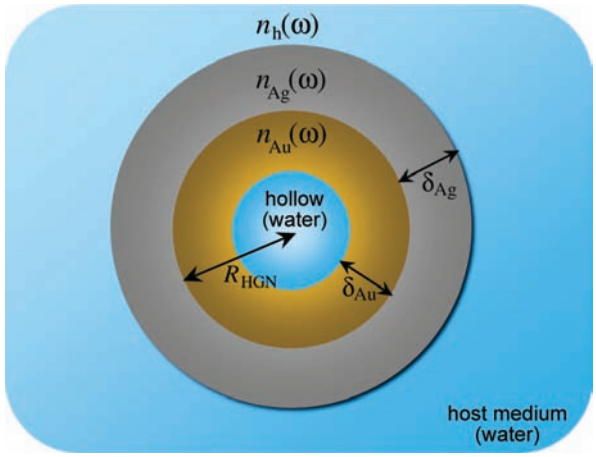

the quasi-static limit. This means that it can be applied to small NPs (<40 nm) where light scattering can be neglected. In contrast, this work does not use such an approximation, so that our model can be applied to NPs of arbitrary size.

Results and Discussion

Hollow polycrystalline nanospheres can be experimentally synthesized using a technique called galvanic replacement. As the metal ions interact with the surface of NPs of another metal, the metal ions can be reduced into metal while the original metal nanoparticles are oxidized into metal ions due to their difference in redox potentials. In the case of the work of Xia et al., silver particles formed are used as the "template" and gold ions are added to the solution.[38−40] One remarkable feature is that this approach can be applied to almost any shape of nanostructures such as hollow rods, spheres, rattles, cubes, and wires.

Recently, a similar approach has been used to produce highly uniform hollow gold nanospheres (HGN) with tunable optical properties.[31,32] It was possible to tune the plasmon absorption in the entire visible and near-IR region of the spectrum by simply controlling the shell thickness and sphere diameter. While the HGNs are indeed very uniform, they provide relatively weak surface-enhanced Raman spectra (SERS) signal compared to solid Ag nanoparticles. Ideally, one would produce hollow silver, instead of gold, nanospheres to improve their SERS sensitivity. However, using the galvanic replacement procedure, it is impossible to produce homogeneous particles. In order to get around this, recently, it was possible to cap very thin HGNs with silver using the seed mediate growth method.[33]

Therefore, we are interested in studying hollow gold−silver nanospheres immersed in water, as shown in Scheme 2, where δ_{Ag} and δ_{Au} denote the thickness of the silver and gold shells, with refraction indexes $n_{Ag}(\omega)$ and $n_{Au}(\omega)$, respectively. The parameter R_{HGN} give us the radius of the hollow gold NP that is used as the seed and is coated with silver. The physical model simulates the recently synthesized NPs,[33] whose SPRs were tuning by changing the parameters: R_{HGN}, δ_{Ag}, and δ_{Au}. Our purpose here is to find if this model, using the extended Mie theory, can simulate the general behavior of the experimental data and to understand the physical origin of the response of the SPRs. In this work we use the size-corrected refraction indexes of Ag and Au.[1] The experimental data were taken from ref 41, and the surface damping was introduced according to Kreibig.[42]

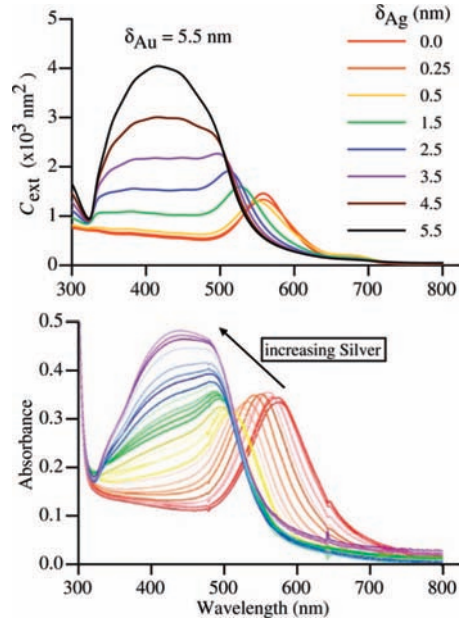

Figure 1. Calculated C_{ext} of a hollow gold−silver double-shell spherical NP immersed in water with R_{HGN} = 14 nm, varying δ_{Ag} from 0 to 5.5 nm, and a fixed δ_{Au} = 5.5 nm (top plot). Experimentally measured absorbance of a HGN of 14 nm radius, with δ_{Ag} coverage from 0 to ~3.5 nm and δ_{Au} ~ 5.5 nm (bottom plot). The experimental data are reprinted with permission from ref 33. Copyright 2008 American Chemical Society.

Surface Plasmons in Hollow Gold−Silver Double-Shell Nanoparticles. To reproduce the experimental findings in hollow gold−silver double-shell nanoparticles,[33] we consider a HGN of 14 nm of radius, with a fixed δ_{Au} = 5.5 nm. Then, it is coated with silver where δ_{Ag} takes values from 0 to 5.5 nm. In Figure 1, the calculated extinction cross section of the hollow gold−silver NP is shown and compared with the experimental absorbance data from ref 33. The calculated spectrum of the seed HGN shows a SPR at 560 nm (red line), which is red-shifted from the one corresponding to a solid gold nanosphere in water (~520 nm).[31] As δ_{Ag} increases the SPR of the hollow gold−silver double-shell NP can be tuned from the HGN resonance to the silver NP plasmon band, which is at shorter wavelengths. At the beginning, the SPR of the HGN is blue-shifted as δ_{Ag} increases, then at a given size (δ_{Ag} ~ 2.5 nm) a second peak is now evident at about 400 nm. For larger δ_{Ag}, the first peak is no longer blue-shifted and reaches a limit at about 500 nm, while the peak at 400 nm increases as δ_{Ag} does, such that, an anisotropic wide peak dominates the spectrum. The calculations are consistent with the measured absorbance for HGN as silver is added in 10−20 μL increments from beginning to end of the coated process.[33] The overall behavior of the experimental data is well reproduced by our calculations. However, there are discrepancies in the position, width, and line shape between the calculated and experimental spectra. These discrepancies can be attributed to several possible factors, e.g., small changes of the refraction index of the host medium, approximations made in the theoretical refraction indexes, and inhomogeneities in the shell thickness, diameter, and morphology of the experimental samples that deviate from the theoretical model used. On a qualitative or semiquantitative level, the agreement is very good.

The general behavior of the optical properties of metallic multishell NPs is governed by the interaction of the plasmon excitations in each nanoshell with both plasmons on the nearest shells. First, the plasmon of the HGN can be seen as the plasmon

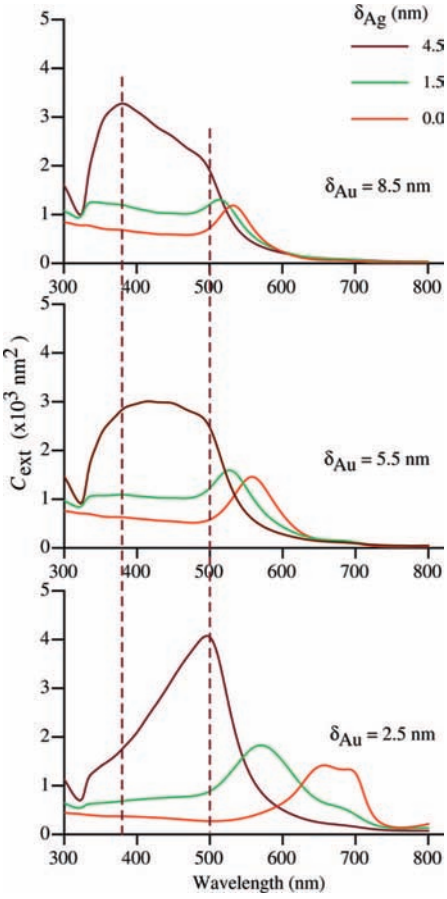

Figure 2. Calculated C_{ext} of a hollow gold−silver double-shell spherical NP immersed in water with $R_{HGN} = 14$ nm, varying δ_{Ag} from 0 to 4.5 nm. Top panel with $\delta_{Au} = 8.5$ nm, midpanel with $\delta_{Au} = 5.5$ nm, and bottom panel with $\delta_{Au} = 2.5$ nm.

hybridization of the two free excitations of the cavity and the sphere, as observed in the quasi-static limit case.[37] In this limit, it has been found that the energy and strength of the resulting plasmon hybridization depend on the aspect ratio (a.r.) of the Au thickness and the hollow radius, i.e., a.r. $= \delta_{Au}/R_{HGN}$, and on the energy of the free plasmons, which in turn are given by the dielectric properties of both hollow and sphere. As smaller a.r., the plasmon interaction increases shifting the hybridized resonance to larger wavelengths. This means that it is possible to tune the optical response of the seed HGN in water or other host medium by changing, for instance, δ_{Au}, and then it is possible to modulate this SPR by using Ag shells of different thicknesses, as we show in the following.

Tuning Surface Plasmons in Hollow Gold−Silver Double-Shell Nanospheres. In Figure 2, C_{ext} spectra for HGNs with $R_{HGN} = 14$ nm, three different δ_{Au} (=2.5, 5.5, and 8.5 nm) with Ag coverage of 0, 1.5, and 4.5 nm are shown. The SPR maxima of the HGN (red curves) move from 660 to 530 nm by increasing δ_{Au} from 2.5 to 8.5 nm. It is interesting to notice that even as both the amount of gold and the absorption increase, the SPR is dependent on the a.r. and is more intense for the case of smallest a.r. $= 2.5/14 = 0.178$. This is because the interaction among surface plasmons in both sides of the shell is stronger for smaller a.r. When the HGN is covered with Ag, the SPR is blue shifted, the peak is wider, and the absorption becomes more intense; again due to the interaction between the plasmons in both sides of the two shells. As δ_{Au} becomes smaller, the blue shift becomes larger. A small peak is observed at about 700 nm for all the spectra, and it is more visible in the bottom panel, such that it looks like the SPR is split. However, this peak is an artifact of the calculation due to the low density of experimental data from where the dielectric properties of bulk Au were taken.[41]

In Figure 2 one can identify three different steps in the evolution of the SPRs: (i) the interaction of both plasmons on Au that depends on the thickness of the shell. (ii) The plasmon interactions between Au and Ag shells that moves the SPR to shorter wavelengths, reaching a limit around 500 nm. This can be observed for all the hollow gold−silver double-shell NP independently of the thickness of the Au shell. However, the strength of the plasmon interactions between Ag and Au shells depends on their thickness, in such a way that the peak at 500 nm is more intense for smaller δ_{Au}. Finally, at a given Ag coverage (iii) the interaction of both plasmons on the Ag shell starts to be present and eventually (with $\delta_{Ag} > 3.5$ nm) dominates at wavelengths shorter than 400 nm. Once the SPR at 500 nm has reached a limit, the other resonance below 400 nm is still growing as δ_{Ag} increases. The growth of this SPR associated to the silver shell depends on the thickness of the Au shell and then on the surface plasmon interactions of both shells. For instance, for the larger thickness $\delta_{Au} = 8.5$ nm the interaction with the plasmon on the Au shell is weaker and the SPR below 400 nm is more intense (top panel). However, as δ_{Au} diminishes, the interaction modulates the strength of the SPR at 400 nm and for $\delta_{Au} = 5.5$ nm and $\delta_{Ag} = 4.5$ nm the intensities of both Au and Ag shell SPRs are the same, while for $\delta_{Au} = 2.5$ nm and $\delta_{Ag} = 4.5$ nm the SPR at 500 nm still dominates the spectrum. The interaction of the plamons with different combination of Ag and Au shell thickness allows us to tune the SPRs. The variation of the profile of the SPR spectra can be reasonably described within the plasmon hybridization model since the light scattering by these NPs is small.[37]

Shape Effects on the Surface Plasmons in Hollow Gold−Silver Double-Shell Nanospheres. The growth of nanoshells induces stress in the inner and outer NP's faces, producing HGN and double-shell NPs that are not single crystals.[31,33] While there are single crystal domains, there is significant twinning when the entire shell is examined closely. The shell is apparently polycrystalline, as is likely true for most to date. The same was observed for double-shell NPs,[33] where it is extremely challenging, if possible at all, to produce a shell that is entirely single crystalline. Structural characterization at the atomic scale is essential for nanomaterials. Lack of a detailed structural study can often lead to controversies regarding proper identification of their properties. To explore the influence of the structural details, we have calculated the extinction cross section of an icosahedral double-shell NP. Because of the complexity of the system, we employ the discrete dipole approximation (DDA), which has been used to study a wide variety of nanoparticles.[4,23,43] A complete explanation of the DDA method can be found elsewhere,[23] here we only discuss the results obtained.

In Figure 3, the extinction cross section of a hollow gold−silver double-shell NP with icosahedral shape is shown. We consider an initial HGN of 28 nm of diameter with a fixed shell $\delta_{Au} = 5.5$ nm, and coated with silver, where δ_{Ag} takes values from 0 to 5.5 nm. Comparing with the top plot in Figure 1, where a similar calculation using the extended Mie theory developed here was done, we observe the following. The general behavior is the same for both spherical and icosahedral NPs, although the position, width, and line shape of the spectra show some differences. For example, the position of the SPR of the HGN of the icosahedral NP is red shifted with respect to

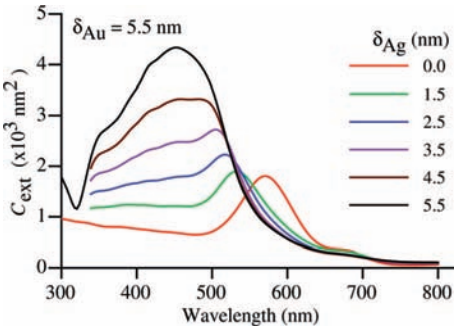

Figure 3. Calculated C_{ext} of a hollow gold−silver double-shell icosahedral NP immersed in water with different δ_{Ag} from 0 to 5.5 nm, and $\delta_{Au} = 5.5$ nm.

that of the spherical NP by about ∼15 nm, being closer to the experimental value (∼610 nm).[33] The SPR is moved to shorter wavelengths as δ_{Ag} increases, at the same time that secondary SPRs appear from 350 to 450 nm, the latter dominate the spectra for large thicknesses δ_{Ag}. One important difference between spherical and icosahedral NPs is that for the later the SPR peak at longer wavelengths, which is associated to the HGN, does not reach a limit at 500 nm as for the case of spherical NPs. The same happens with the second peak associated to the Ag shell, which does not reach also a limit at 400 nm as for the spherical NP. This comportment can be attributed to the different number and position of the SPRs between spherical and icosahedral NPs, which makes the spectra of icosahedral morphologies look more anisotropic than those for spherical NPs.[1,23]

Notice that the plasmon lifetime as well as the measured SPR bandwidth can be influenced by the presence of twins in the NP. For that reason, we have employed again the simple approximation to take into account this effect by introducing an effective conduction electron mean free path for a spherical nanoparticle.[42] We should keep in mind that although the bandwidth depends on the arbitrary shape of the nanoparticle,[44] the location of the SPRs does not change.[1]

Gold-Core Silver-Shell Nanoparticles. To show the versatility of hollow gold−silver double-shell nanoparticles as compared with similar structures, here we present results for gold-core silver-shell nanospheres. Two gold-core sizes with different thicknesses of silver shells were studied. In Figure 4, the extinction cross section spectra of gold-core silver-shell NPs are shown for two different sizes of the solid core of 35 (top) and 48 nm (bottom) and a silver shell of thickness δ_{Ag} that varies from 0 to 7 nm. The nanoparticle is immersed in water as before. As expected when $\delta_{Ag} = 0$, the SPR of the solid gold NP is fixed at about 525 nm for the sizes studied here. In contrast, the SPR of the HGN can be tuned by varying the thickness of the gold shell, as shown previously. Now, when a silver shell is grown over the solid gold core, the original SPR is blue shifted, and at about 500 nm it reaches its limit again. Simultaneously, a second SPR emerges at around 380 nm and becomes more intense as δ_{Ag} increases. The overall behavior is similar to that found in hollow gold−silver double-shell NPs, although the range of accessible wavelengths of the SPRs is narrower, in particular in red region of the EM spectrum. The intensities of the SPRs at 400 and 500 nm depend on the solid core size, as it happens also for the HGN. However, in this case, as the solid gold core becomes larger, the interaction with the silver shell is stronger. Again, the aspect ratio between the core size and the thickness of the silver shell plays an important role.

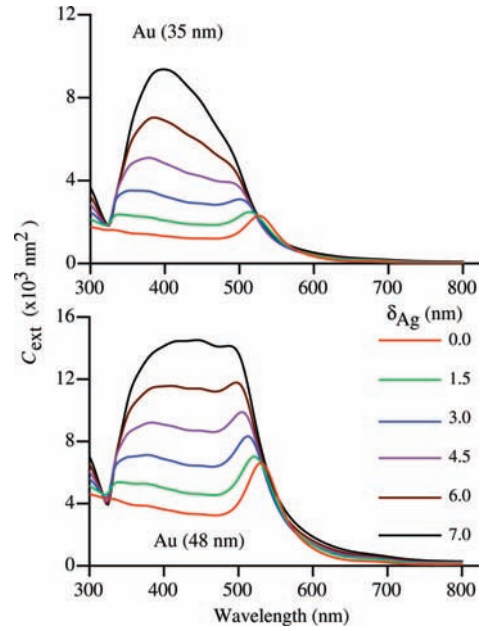

Figure 4. Calculated C_{ext} of gold−silver core−shell spherical NPs immersed in water with core diameter of 35 (top) and 48 nm (bottom), with different δ_{Ag} from 0 to 7 nm.

Conclusions

An extended Mie theory was developed to study the optical properties of multiconcentric metallic-shell nanoparticles. The theory reproduces very well recent experiments of the optical absorbance of hollow gold−silver double-shell nanospheres as a function of the silver-shell thickness.[33] The optical absorption is mainly characterized by two surface plasmon resonances. The first SPR band is due to the seed hollow gold nanospheres. The position and intensity of this SPR band depend on the aspect ratio of the hollow and gold shell, with thinner gold shells corresponding to more red-shifted SPR. The second SPR band at shorter wavelength is due to the Ag shell on top of the gold shell, which becomes more intense as the silver shell thickness increases. The first resonance reaches a limit at a wavelength that depends on the dielectric properties of both shells, in this case at 500 nm. The growth rate of the second resonance depends on both silver and gold shell thicknesses. As the silver-shell thickness increases, both resonances are close enough and a wide absorption feature is always observed. Using the discrete dipole approximation, the optical response of a hollow gold silver double-shell icosahedral nanostructure is also studied. It is found that the nanoparticle's shape is an important factor that has to be taken into account to clearly identify and understand the behavior of the surface plasmon resonances in these multishell nanostructures. It was shown that the extended Mie theory, to a good approximation, provides a reasonable description of the experimentally observed SPR in a hollow gold−silver double nanoshells. The numerical calculations are useful to better understanding key factors that affect the SPR in such complex structures. These types of multishell spherical metal nanostructures are promising for applications in SPR detection and imaging, SERS, sensing, and nanophotonics and for biomedical applications

Appendix

To find the solutions of the scattered electromagnetic field of eqs 2, given in terms of the Debye potentials, we have followed the formalism developed in ref 36 for the calculation

of the optical response of one spherical shell. Here, we generalized the Mie theory[35] by considering a spherical nanoparticle composed by a set of N concentrical spherical surfaces with radii R_i and different dielectric properties n_i, which is immersed in a host medium, as we have described in section II. The independent Debye potentials $\Psi^{(e)}$ and $\Psi^{(m)}$ satisfy the scalar Hemholtz equation

$$\nabla^2\Psi_i^{(e/m)} + k^2\Psi_i^{(e/m)} = 0 \quad (7)$$

which has solutions that can be written as the sum of spherical harmonic multipolar functions

$$\Psi_i(r,\theta,\varphi) = \sum_{l=0}^{\infty}\sum_{m=-l}^{l}\{A_{l,m}{}^i h_l(kr) + B_{l,m}{}^i j_l(kr)\}P_l^m(\cos\theta)e^{im\varphi} \quad (8)$$

with $i = 1,..., N$, and where $h_l = j_l + iy_l$ are the spherical Hankel functions and j_l and y_l are the spherical Bessel functions of the first and second kind, respectively. For example, consider a plane wave that propagates in the $\theta = 0$ direction and is polarized along $\theta = 90°$ and $\varphi = 0°$ direction, such that, the harmonic function expansions of its Debye potentials are

$$\Psi^{(e)}(r,\theta,\varphi) = \sum_{l=1}^{\infty} i^{l-1}\frac{2l+1}{l(l+1)}j_l(kr)P_l^1(\cos\theta)\cos\varphi \quad (9)$$

$$\Psi^{(m)}(r,\theta,\varphi) = \sum_{l=1}^{\infty} i^{l}\frac{2l+1}{l(l+1)}j_l(kr)P_l^1(\cos\theta)\sin\varphi \quad (10)$$

The electromagnetic field in eqs 2 and 3 must satisfy the boundary conditions at each surface of radius R_i with $i = 1, 2,..., N$, i.e.

$$(\mathbf{E}_{(i)} - \mathbf{E}_{(i+1)})\times\hat{\mathbf{e}}_r = (\mathbf{H}_{(i)} - \mathbf{H}_{(i+1)})\times\hat{\mathbf{e}}_r = 0 \quad (11)$$

where $\hat{\mathbf{e}}_r$ is the unitary vector along the radial direction in spherical coordinates. The above equations give us the boundary conditions on the Debye scalar potentials, which consist in the continuity of the functions for the magnetic potential

$$n_i^2(\omega)\Psi_i^{(e)} \quad \text{and} \quad \frac{\partial}{\partial r}[r\Psi_i^{(e)}] \quad (12)$$

and for the electric potential

$$\Psi_i^{(m)} \quad \text{and} \quad \frac{\partial}{\partial r}[r\Psi_i^{(m)}] \quad (13)$$

These boundary conditions relate the coefficients of the potential of the ith shell with all the interior shells. Thus, one obtains a set of four equations for the ith spherical surface, which have the following form

$$a_l{}^i\xi_l(k_iR_i)k_i + b_l{}^i\chi_l(k_iR_i)k_i - a_l{}^{i+1}\xi_l(k_{i+1}R_i)k_{i+1} - b_l{}^{i+1}\chi_l(k_{i+1}R_i)k_{i+1} = 0 \quad (14)$$

$$a_l{}^i\xi_l'(k_iR_i) + b_l{}^i\chi_l'(k_iR_i) - a_l{}^{i+1}\xi_l'(k_{i+1}R_i) - b_l{}^{i+1}\chi_l'(k_{i+1}R_i) = 0 \quad (15)$$

$$c_l{}^i\xi_l(k_iR_i)/k_i + d_l{}^i\chi_l(k_iR_i)/k_i - c_l{}^{i+1}\xi_l(k_{i+1}R_i)/k_{i+1} - d_l{}^{i+1}\chi_l(k_{i+1}R_i)/k_{i+1} = 0 \quad (16)$$

$$c_l{}^i\xi_l'(k_iR_i) + d_l{}^i\chi_l'(k_iR_i) - c_l{}^{i+1}\xi_l'(k_{i+1}R_i) - d_l{}^{i+1}\chi_l'(k_{i+1}R_i) = 0 \quad (17)$$

where we have defined $\xi_l(x) = xh_l(x)$ and $\chi_l(x) = xj_l(x)$, with the prime meaning the derivative with respect to the argument of the function, and $a_l{}^i$, $b_l{}^i$, $c_l{}^i$, and $d_l{}^i$ are the coefficients of the sums given in eqs 4 and 5. Then, one obtains a linear system of $2N - 1$ equations with $2N$ unknown coefficients for each pair of indexes (l, m). Finally, one solves the coefficients considering the orthogonality of the harmonic functions and in terms of the incident EM plane wave. For this, we have taken into account that in the case of well-behaved EM fields, the coefficients $d_l{}^1$ and $b_l{}^1$ should be zero at the origin of our coordinate system, while in the host medium, i.e., in $r > R_N$, the coefficients $b_l{}^{N+1}$ and $d_l{}^{N+1}$ correspond to those of the incident EM wave, while $a_l{}^{N+1}$ and $c_l{}^{N+1}$ correspond to the scattered ones. Then, one finally arrives at the expression for the extinction cross section given in eq 6, which can be solved numerically for a NP composed by an arbitrary number of shells.

Acknowledgment. C.N. is grateful to CONACyT and DGAPA-UNAM for financial support under Grants No. 48521 and No. IN106408, respectively. J.Z.Z. is grateful to the US NSF and NASA UARC for support.

References and Notes

(1) Noguez, C. *J. Phys. Chem. C* **2007**, *111*, 3806.
(2) Zhang, J. Z.; Noguez, C. *Plasmonics* **2008**, *3*, 127.
(3) Kelly, K. L.; Coronado, E.; Zhao, L. L.; Schatz, G. C. *J. Phys. Chem. B* **2003**, *107*, 668.
(4) González, A. L.; Ortiz, G. P.; Rodríguez-Gattorno, G.; Noguez, C. *J. Phys. Chem. B* **2005**, *109*, 17512.
(5) Abiko, F.; Tomoo, K.; Mizuno, A.; Morino, S.; Imataka, H.; Ishida, T. *Biochem. Biophys. Res. Commun.* **2007**, *355*, 667.
(6) Chen, L. L.; Deng, L.; Liu, L. L.; Peng, Z. H. *Biosens. Bioelectron.* **2007**, *22*, 1487.
(7) Du, X. Z.; Wang, Y. C. *J. Phys. Chem. B* **2007**, *111*, 2347.
(8) Dong, H.; Cao, X. D.; Li, C. M.; Hu, W. H. *Biosens. Bioelectron.* **2008**, *23*, 1055.
(9) Li, Y.; Lee, H. J.; Corn, R. M. *Nucleic Acids Res.* **2006**, *34*, 6416.
(10) Fleischmann, M.; Hendra, P. J.; McQuillan, A. *J. Chem. Phys. Lett.* **1974**, *26*, 163.
(11) Albrecht, M. G.; Creighton, J. A. *J. Am. Chem. Soc.* **1977**, *99*, 5215.
(12) Jeanmaire, D. L.; Vanduyne, R. P. *J. Electroanal. Chem.* **1977**, *84*, 1.
(13) Moskovits, M. *J. Chem. Phys.* **1978**, *69*, 4159.
(14) Michaels, A. M.; Jiang, J.; Brus, L. *J. Phys. Chem. B* **2000**, *104*, 11965.
(15) Melancon, M. P.; Lu, W.; Yang, Z.; Zhang, R.; Cheng, Z.; Elliot, A. M.; Stafford, J.; Olsen, T.; Zhang, J. Z.; Li, C. *Mol. Cancer Ther.* **2008**, *7*, 1730.
(16) Lu, W.; Xiong, C.; Zhang, G.; Huang, Q. ; Zhang, R. ; Zhang, J. Z.; Li, C. 2008, in press.
(17) Henglein, A. *Chem. Rev.* **1989**, *89*, 1861.
(18) Pileni, M. P.; Taleb, A.; Petit, C. *J. Dispersion Sci. Technol.* **1998**, *19*, 185.
(19) Emory, S. R.; Nie, S. *J. Phys. Chem. B* **1998**, *102*, 493.
(20) Heilmann, A.; Kreibig, U. *Eur. Phys. J., Appl. Phys.* **2000**, *10*, 193.
(21) Lazarides, A. A.; Kelly, K. L.; Jensen, T. R.; Schatz, G. C. *J. Mol. Struct.: THEOCHEM* **2000**, *529*, 59.
(22) Zhang, J. Z.; Wang, Z. L.; Liu, J.; Chen, S.; Liu, G.-y. *Self-assembled Nanostructures*; Kluwer Academic/Plenum Publishers: New York, 2003.
(23) González, A. L.; Noguez, C. *J. Comput. Theor. Nanosci.* **2007**, *4*, 231.
(24) Norman, T. J.; Grant, C. D.; Magana, D.; Zhang, J. Z.; Liu, J.; Cao, D. L.; Bridges, F.; Van Buuren, A. *J. Phys. Chem. B* **2002**, *106*, 7005.
(25) Murphy, C. J.; San, T. K.; Gole, A. M.; Orendorff, C. J.; Gao, J. X.; Gou, L.; Hunyadi, S. E.; Li, T. *J. Phys. Chem. B* **2005**, *109*, 13857.
(26) Gou, L. F.; Murphy, C. J. *Chem. Mater.* **2005**, *17*, 3668.
(27) Murphy, C. J.; Sau, T. K.; Gole, A.; Orendorff, C. J. *MRS Bull.* **2005**, *30*, 349.
(28) Nikoobakht, B.; El-Sayed, M. A. *Chem. Mater.* **2003**, *15*, 1957.
(29) Sun, Y. G.; Mayers, B. T.; Xia, Y. N. *Nano Lett.* **2002**, *2*, 481.
(30) Sun, Y. G.; Mayers, B.; Xia, Y. N. *Nano Lett.* **2003**, *3*, 675.

(31) Schwartzberg, A. M.; Olson, T. Y.; Talley, C. E.; Zhang, J. Z. *J. Phys. Chem. B* **2006**, *110*, 19935.
(32) Schwartzberg, A. M.; Grant, C. D.; van Buuren, T.; Zhang, J. Z. *J. Phys. Chem. C* **2007**, *111*, 8892.
(33) Olson, T. Y.; Schwartzberg, A. M.; Orme, C. A.; Talley, C. E.; O'Connell, B.; Zhang, J. Z. *J. Phys. Chem. C* **2008**, *112*, 6319.
(34) *Absorption and Scattering of Light by Small Particles*; Bohren, C. F., Human, D. R. , Eds.; John Wiley & Sons: New York, 1983.
(35) Mie, G. *Ann. Phys.* **1908**, *25*, 377.
(36) Born M.; Wolf, E.; *Principles of Optics*; Cambridge University Press: Melbourne, 1999.
(37) Prodan, E.; Nordlander, P. *J. Chem. Phys.* **2004**, *120*, 5444.
(38) Sun, Y. G.; Mayers, B.; Xia, Y. N. *Adv. Mater.* **2003**, *15*, 641.
(39) Sun, Y. G.; Wiley, B.; Li, Z. Y.; Xia, Y. N. *J. Am. Chem. Soc.* **2004**, *126*, 9399.
(40) Wang, C. H.; Sun, D. C.; Xia, X. H. *Nanotechnology* **2006**, *17*, 651.
(41) Johnson, P. B.; Christy, R. W. *Phys. Rev. B* **1972**, *6*, 4370.
(42) Kreibig, U. *J. Phys. F: Met. Phys.* **1974**, *4*, 999.
(43) González, A. L.; Reyes-Esqueda, J. A.; Noguez, C. *J. Phys. Chem. C* **2008**, *112*, 7356.
(44) Coronado, E. A.; Schatz, G. C. *J. Chem. Phys.* **2003**, *119*, 3926.

JP810422R